5524 *Macromolecules* **2010**, *43*, 5524–5529
DOI: 10.1021/ma100233r

Macromolecules
ARTICLE

Droplet-Based Millifluidics as a New Miniaturized Tool to Investigate Polymerization Reactions

Nicolas Lorber, Bertrand Pavageau, and Emmanuel Mignard*

CNRS-Rhodia-Université Bordeaux 1, UMR5258 Laboratoire du Futur, 178 Av. Dr. Albert Schweitzer, 33608 Pessac Cedex, France

Received January 29, 2010; Revised Manuscript Received May 20, 2010

ABSTRACT: We present herein an original tool to monitor polymerization kinetics. It consists in a droplet-based millifluidic approach where the use of aqueous droplets of monomer can be seen as polymerization microreactors. Acrylic acid mixed with sodium persulfate at low pH was used as a fast and exothermic polymerization model. By using a nonintrusive spectroscopic system with our millifluidic system, we were able to safely investigate harsh polymerization conditions. As expected, polymerizations exhibited higher order with respect to monomer concentration than the usual first-order kinetics for ideal free-radical polymerization, and a $^1/_2$ dependence with respect to the initiator concentration. The overall activation energy for polymerization rate was also estimated to 47.0 kJ mol^{-1}. Also, it has been shown that E_r becomes temperature dependent due to the solution viscosity, i.e., low temperatures and high concentrations. These results set the stage for further studies of polymerization reactions where detailed basic kinetic data must be acquired in conditions which cannot be investigated by using conventional batch glassware, i.e., high temperatures or concentrations. This versatile approach can also be used as an efficient high throughput screening tool.

Introduction

Reactions in droplets in microfluidic channels is an attractive approach which is based upon micromanipulation of discrete droplets.[1,2] To the chemist, the main advantage by using theses droplets is they can be used as individual batch microreactors. Recently, this approach was used in order to synthesize polymeric particles like latex, vesicles, hybrids, Janus, etc.[3,4] Droplets are easily generated by using flow focusing or simple T junction patterns and at least two immiscible fluids. One of these can be a chemically inert carrier fluid (usually silicon or fluorinated oils). Thus, a string of aqueous droplets flows continuously within channels or tubes. There are many advantages in using these small droplet-based systems.[1,2] First, by using the same experimental conditions to generate these droplets, i.e., constant flow rates, flow patterns, etc., these microreactors will have the same size and shape and will contain the same chemical composition. Hence, all the microreactors generated during the experiment will be identical, at least until flow rates remain the same. By varying flow rates from the feed stock solutions one can easily control the chemical composition of these microreactors. Moreover, according to viscosities and surface tensions of fluids, chaotic advections can enhance internal mixing of the droplets.[2,5,6] On the other hand, due to their small sizes and high surface-area-to-volume ratios, heat exchanges are favored which improves safety at the laboratory. This advantage thanks to the miniaturization of the process is an important feature in polymerization: one can make polymerization reactions with experimental conditions which could be difficult to use in conventional batch reactors, i.e., high concentrations or temperatures. For instance, although J. Yoshida et al. did not use droplets in their pioneer works but a continuous flow of monomer mixed with the initiator, the authors proved that small tubular microreactors are efficient for controlling highly exothermic free radical polymerization.[7] Here, in contrast to single-phase flows, other key characteristics to this miniaturized droplet-based approach consist of the fact that (1) droplets can manage high internal viscosity issues without plugging the channel and (2) dispersion due to convection and diffusion is eliminated because the reactants are compartmentalized within droplets. Since all droplets move at the same speed, they do not coalesce and there is no residence time distribution.[8] This is particularly important since viscosity in polymerization reactions can increase to thousand of centipoises or even higher in the case of gel processes. The consequence of using this droplet approach is that there is equivalence between the position of the droplet within the channel and the time course of the reaction: i.e., according to the rate of the reaction, each droplet will have the same chemical composition when the droplet reaches the same position along the channel. This is of particular interest in order to acquire basic kinetic data.

Moreover, the transparency of the walls of the channels allows using nonintrusive optical techniques to observe the behavior of the droplets or spectroscopies to analyze their compositions. For instance, K. L. Beers et al. used Raman spectroscopy in order to monitor benzyl methacrylate conversion.[9] Droplets of various monomer compositions were generated by using a flow focusing technique, and then were photopolymerized in a thiolene-based microfluidic device. This process eliminates the tedious sampling and handling like extraction, dilutions or filtrations, etc. which are required by HPLC or GC for instance. Moreover, such chromatographic systems or nuclear magnetic resonance instruments are usually costly to implement and maintain. Hence, this in line monitoring is a faster and cheaper method than the other ones used in order to obtain residual concentrations of the monomer as a function of time. By using this in line monitoring capacity and the time-space equivalence, one can determine concentrations at any time of the reaction.[10] Kinetics of very fast polymerization reactions which are done in few minutes can be determined safely. Moreover, since this approach is a

*Corresponding author. Telephone: +33 5 5646 4732. Fax: +33 5 5646 4790. E-mail: emmanuel.mignard-exterieur@eu.rhodia.com.

 Published on Web 06/02/2010

nondestructive one, one can recover the product at the outlet of the device for subsequent analyses.

According to the reaction speed, or to the availability of reagents, such a miniaturization to the fabrication of microfluidic devices is not necessary. Indeed, microfluidics is based on expensive microfabrication technologies which require a high know-how and expertise.[4] And more the microchannel pathway is complex and more the risk of failed in realizing the microchip could be important. This is a time and money consuming process which can be avoided. Hence, we set up and use a miniaturized tool at a scale higher than that one commonly used in microfluidics: it consists in assembling Teflon tubing of about the millimeter with commercial connectors. This millifluidic approach is cheaper since it does not need the use of expertise in microfabrication neither a clean room. It is faster to set up and more flexible than microfluidic devices since one can use again the tubing in other configurations, i.e., length path, diameter size, etc. The laboratory has patented this droplet-based millifluidic reactor.[11−13] We used it to produce continuously isometric particles made from Noa polymer or porous silica with a high control of their sizes (from 100 μm to few millimeters) and shape (spherical to ovoid).[14,15] By using simple coaxial tubing, stable emulsions were obtained without the need of surfactants.[16] This tool was also used to monitor the kinetics of the redox synthesis of iodine by UV−visible spectroscopy.[17] Other groups have also used with success this transparent droplet-based millifluidic approach. For instance, from micrometer- to millimeter-sized monodisperse polymer beads or capsules were fabricated by using respectively interfacial polymerization,[18] or photopolymerization.[19] M. T. Gokmen et al. obtained highly porous polymer particles from the photopolymerization of high internal phase emulsion droplets.[20] Although Z. T. Cygan et al. fabricated thiolene-based devices instead of using Teflon tubes, they used with success this droplet-based millifluidic approach in organic chemistry.[21] And G. Guan et al. used a transparent tubing to monitor the transesterification of sunflower oil to fatty acid methyl ester.[22]

We present herein the use of an original droplet-based millifluidic tool in order to monitor in situ thermally initiated polymerization reactions by confocal Raman spectroscopy. We choose to use experimental conditions where fast and exothermic polymerization process occurs and/or viscosity can be an issue. Acrylic acid (AA) at low pH and high concentrations is hence a good candidate to obtain such behavior.

Materials and Methods

Reagents. Filtered water at 18.2 MΩ·cm (at 25 °C) was obtained from the Synergy unit (Millipore) in which a 0.22 μm pore diameter is mounted. AA (Merck, >99%), potassium nitrate (KNO_3, VWR Normapur, 99%) and sodium peroxodisulfate as the initiator (I_2, VWR Normapur, 99%), were use as received. Aqueous solutions of monomer or initiator were deoxygenated by nitrogen flush prior to use (about 30 min). In our case, droplets are about stable water-in-fluorinated oil emulsions without the need of surfactants. Fluorinated oil FC-40 from 3 M was used as the carrier fluid without further purification.

Set Up of the Millifluidic Device. The millifluidic system is based on commercial tubes and fittings available from Upchurch. Briefly, as shown in Figure 1 the main part of the device consists in a 5 m long FEP tube ($^1/_8$ in. o.d. with $^1/_{16}$ in. i.d.) rolled up in part on a metallic cylinder. This is defined as the tubular reactor. At the inlet of the tube, a coaxial dual tubes was use to generate droplets as previously published.[14−17] High precision syringe pumps (neMESYS from Cetoni) were used to feed the tubular reactor. Inside the metallic support, a cooling fluid flows against the current of reagents that flowed within the tubular reactor. Temperature of the cooling fluid is controlled by a Lauda thermostat (PROLINE RP845). Polymerization occurs only within the part of the tubular reactor which is heated (about 4.50 m long). As can be seen in Figure 1, a metallic flask protects the heated part of the tube. A window allows having an optical access for analysis. A waste container is connected at the end of the tubular reactor. But any kind of sample recovery system can be mounted.

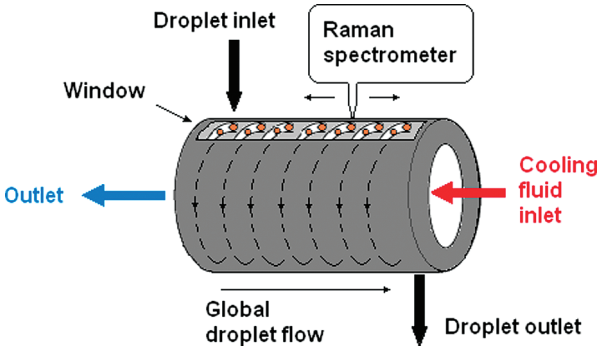

Figure 1. Scheme of the patented millifluidic device.

Table 1. Experimental Conditions for the Polymerization Reactions and Measured $R_{p,0}$

no.	AA[a] w/v % @ t_0	$[AA]_0/[I]_0$[a]	T (°C)	$R_{p,0}$ (mol L^{-1} s^{-1})
1	10	50	72	0.011
2	20	100	72	0.026
3	30	150	72	0.044
4	40	200	72	0.076
5	20	225	72	0.016
6	20	50	72	0.037
7	20	25	72	0.050
8	40	200	63	0.015
9	40	200	67	0.046
10	40	200	76	0.097
11	40	200	80	0.123
12	40	200	88	0.160
13	40	200	95	0.211
14	40	200	98	0.257

[a] Concentrations within the droplets. They are obtained according concentrations of stock solutions and applied flow rates: Q_{oil} = 1190.3 μL·min^{-1}; Q_{AA} = 446.4 μL·min^{-1}; Q_{I_2} = 148.8 μL·min^{-1}; total residence time was 5 min for experiment no. 1 to no. 6 and no. 8, no. 9. For no. 7 and no. 10, Q_{oil} = 2380.6 μL.min^{-1}; Q_{AA} = 892.7 μL.min^{-1}; Q_{I_2} = 297.6 μL.min^{-1}; total residence time was 2.5 min.

Confocal Raman Spectroscopy. The millifluidic device was placed under the confocal microscope of the Raman spectrophotometer (10× objective). Raman scattering spectra were measured through the window of the millifluidic device. They were obtained by a double monochromator Raman spectrometer HR800 (Horiba Jobin-Yvon) with Near Infrared laser diode (785 nm; 300 mW) as excitation source. Note that the spatial resolution of the focused laser beam was about 30 μm in width and 50 μm in depth. The acquisition time for one spectrum was about 90 s (average 2).

Sequence of Operations during Polymerization Monitoring. Aqueous stock solutions of monomer and initiator and the carrier oil were separately prepared and degassed by nitrogen bubbling. Concentrations and other experimental details are given in Table 1. Deoxygenated solutions and the carrier oil were added into degassed syringes mounted on the syringe pump. The carrier fluid syringe is directly connected to the droplet generator while the syringes of the aqueous stock solutions were connected to a homemade miniaturized dynamic stirrer. This system allowed mixing the aqueous stock solution prior the generation of droplets. Before the experiment, the tubular reactor was first equilibrated at room temperature with the carrier oil. The diluted stream of reagents then flowed to the droplet generator system and then to the tubular reactor. Droplets

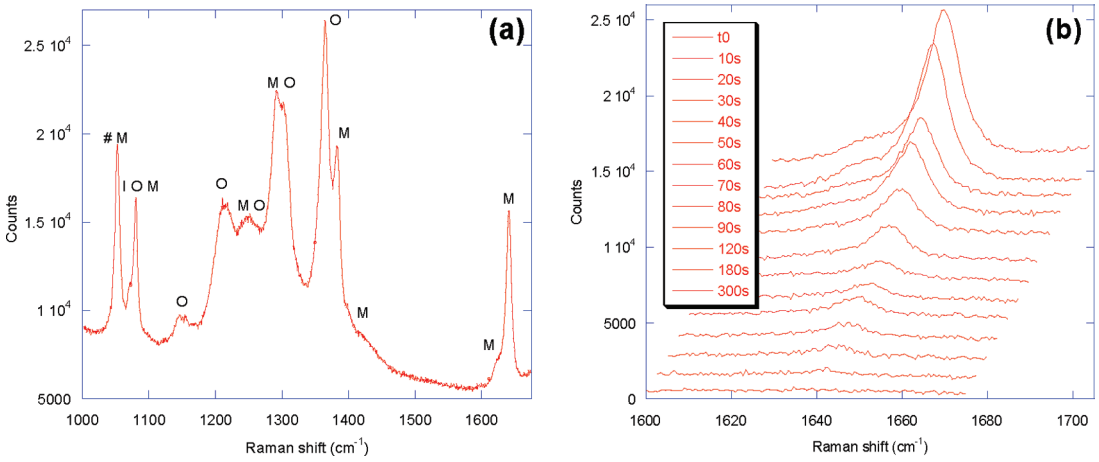

Figure 2. (a) Typical Raman spectrum obtained during the experiment. Peaks are indexed according to the contribution of chemicals (# is KNO_3 (ref); M is AA; I is I_2; O is fluorinated oil). (b) Decrease of the peak corresponding to the conversion of monomer as a function of time.

of diluted AA and initiator solution were formed in order to equilibrate fluid concentrations that were delivered by each syringe. As soon as the equilibrium is reached the Raman spectrum of the initial diluted AA solution was recorded as a reference for the whole experiment. Thus, the time t_0 of the experiment corresponds to this acquisition, whatever the position of the confocal microscope of the Raman spectrometer. Then, the tubular reactor was heated. As soon as the temperature set is reached, we started to record Raman spectra again. During the experiment, constant flow rates were applied in order to set the residence time (t_{rd}) equal to the total time of the polymerization, e.g., $t_{rd} = V_{tube}/Q_{total}$, where V_{tube} is the volume of the tube which is actually heated and Q_{total} is equal to the sum of all applied flow rates. As far as the droplets flow along the heated tubular reactor the polymerization occurs. Since the position x of a droplet within the tubular reactor corresponds to the time course of reaction (t_x), thus each droplet reaching that position are identical in terms of conversions. The relationship between the position and the time course of the reaction is: $t_x = (x\pi r^2)/Q_{total}$, where r is the internal radius of the tube. Recording Raman spectra at different positions along the tubular reactor leads to plot conversion (or concentrations) in function of time. At the end of the experiment, the system was cleaned with the carrier fluid.

Results and Discussion

Typical Raman spectra are shown in Figure 2a. The peak at 1640 cm^{-1} corresponds to the signal of the carbon−carbon double bond of the monomer. As shown in Figure 2b, we monitored the decrease of this peak in function of time (i.e., in function of the position along the flow pathway). Although spectra were obtained while aqueous droplets separated by carrier fluid plugs flowed, their quality is good enough to use them quantitatively: they present a high signal/noise ratio and there is no fluorescence in the analyzed range. However, this acquisition time was long enough that about 850 droplets were analyzed. Thus, the amine oxide Raman scattering at 1050 cm^{-1} from the internal reference KNO_3 was used to normalize each Raman spectrum. Note the relative intensity of the peak of the reference diluted in the aqueous droplets do not significantly varies from one spectrum to another, as expected.

Molar conversion $\rho(t)$ is then calculated according the following equation:

$$\rho(t) = 1 - \frac{n_{AA}(t)}{n_{AA}(t_0)} = 1 - \frac{\dfrac{h_{AA}(t)}{h_{KNO_3}(t)}}{\dfrac{h_{AA}(t_0)}{h_{KNO_3}(t_0)}} \qquad (1)$$

where $h_y(t)$ is the height measured at a time t at the top of the peak corresponding to the chemical y. By assuming concentration is directly proportional to the height of the peak and there is no significant change in the respective Raman spectra of the heated chemicals (i.e., shifting or band broadening), then these height ratios allowing to eliminate all calibration constants. The molar concentration of AA is thus: $[AA]_t = [AA]_0 \cdot [1-\rho(t)]$. By using the law of mass conservation, one can calculate molar PAA concentrations in function of time. As first approximations, we assume an ideal mixing and we have neglected any variation of the volume of the microreactors which occurs during the polymerization reaction due to the difference between the mass densities of the monomer and polymer. As shown in Figure 3, we can plot molar monomer conversion in function of time. This in line monitoring shows polymerization reactions is almost complete at the end of the experiments, meaning the collected droplets are constituted by PAA in solution essentially. In some cases, the polymer concentration could be high, and the corresponding collected droplets look like gels and were difficult to dissolve into water.

Polymerization were done at low pH, and according to the Henderson−Hasselbalch equation, about >99.5% of the AA was nonionized and therefore the chains in solution were preferably in their coiled form. In ideal free-radical polymerization, monomer is consumed by initiation and chain propagation. And according the long chain and the quasi-steady state approximations, one can obtain:[23]

$$-\frac{d[AA]}{dt} = k_p\sqrt{\frac{fk_d[I_2]}{k_t}}[AA] = \alpha[AA]^a \qquad (2)$$

where k_p, k_d, and k_t are the propagation, deactivation, and termination rate coefficients respectively, f the efficiency factor, α the apparent propagation rate coefficient and a the partial rate order of the polymerization reaction with respect to the monomer. Note k_t adheres to the definition use by Odian[23] and is twice less the value used by Dotson et al.[24] By assuming the concentration of the initiator do not vary during the whole experiment, then $[I_2]$ can be replaced by its initial value $[I_2]_0$.

Effect of the initial monomer concentration on the conversion is shown in Figure 3. For an ideal free-radical polymerization where $a = 1$, the integration of eq 2 gives a first order decay of $[AA]$ according to $[AA] = [AA]_0e^{-\alpha t}$. Thus, the molar conversion becomes $\rho(t) = 1 - e^{-\alpha t}$ and is independent of the initial monomer concentration. Even though the overall behavior of each trace shown in Figure 3 resembles that of first order kinetics, the rate increases with an increasing monomer concentration. This indicates a higher than first order kinetics. From these plot one can obtain the initial rate of polymerization, $R_{p,0}$. Their values are

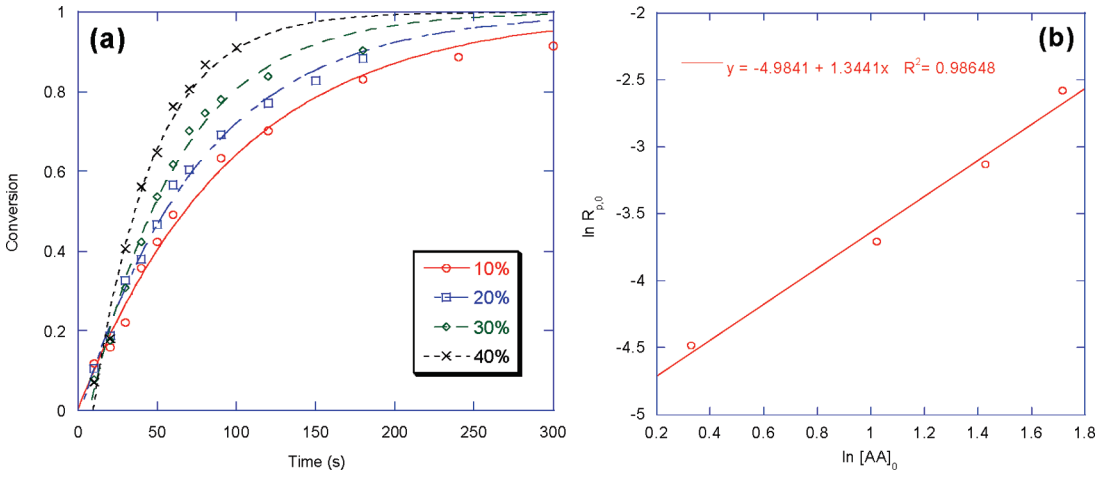

Figure 3. (a) Molar conversions in function of time for different initial monomer concentrations ($[I]_0$ = 0.028 mol·L^{-1} at pH 1.8 and 72 °C). For illustration, data were fitted by using a first-order with respect to initial monomer concentration. (b) Logaritmic representation of $R_{p,0}$ as a function of $[AA]_0$.

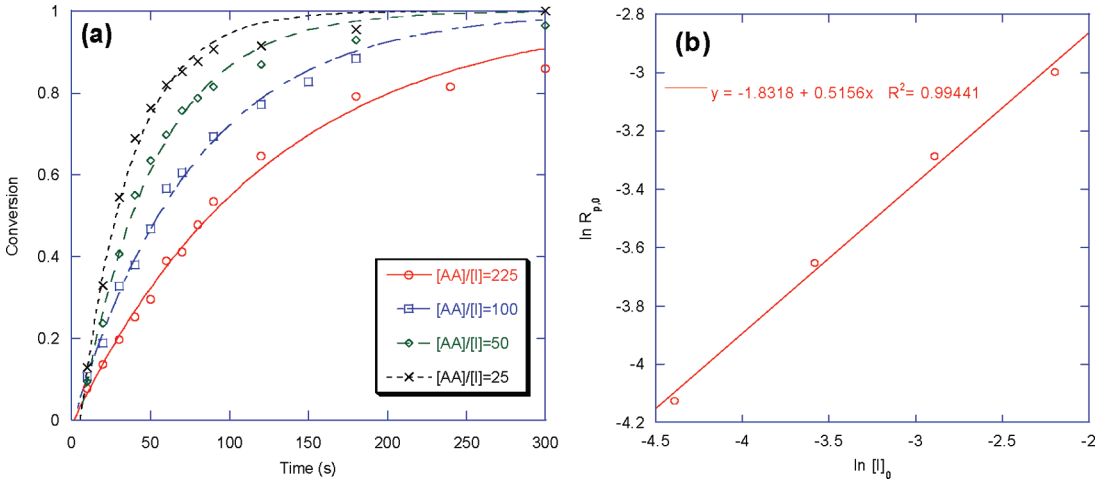

Figure 4. (a) Molar conversions of AA in function of time for several initial initiator concentrations ($[AA]_0$ = 2.8 mol·L^{-1} at pH 1.8 and 72 °C). (b) Logarithmic representation of $R_{p,0}$ in function of $[I]_0$.

reported in Table 1 for each experiment. The slope of the trace ln $R_{p,0}$ in function of ln $[AA]_0$ gives the order of the polymerization rate with respect to monomer concentration and is 1.35 with a correlation coefficient of 0.986. This higher than first order rate is in rather good agreement with previous published works, where orders of AA radical polymerization rates in aqueous solution vary from ~1.0[25,26] to 1.7.[27,28] It was assumed the polymerization kinetics should obey a $^3/_2$ order with respect to the monomer due to side reactions like secondary monomer-enhanced decomposition step of the initiator.[29] On the other hand, one could expect a gel effect should occur since we investigated AA polymerizations at elevated initial monomer concentrations. Scott and Peppas have shown this gel effect does not occurs when unneutralized AA is polymerized at concentrations below 50 wt %.[26] This phenomenon is difficult to detect on our kinetic plots. More points per experiments must be acquired in order to observe such a behavior.

Effect of initial initiator concentration on the conversion is shown in Figure 4a. Again, first-order fits are used for illustration only. As expected, the rate increases with an increasing initiator concentration. Figure 4b also shows the log−log representation of the initial polymerization rate versus the initial initiator concentrations. The trace is quite linear with a slope of 0.52 and the linear regression gives R^2 = 0.994. This result is consistent with an $^1/_2$-order with respect to the initial initiator concentration. This behavior was expected and is in good agreement with the literature.[25−28]

With the droplet-based millifluidic approach, it is very easy to investigate quickly several temperatures without preparing other sets of monomer or initiator solutions. Indeed, only small amounts of stock solutions are needed to perform one experiment. Since the stock solutions are kept at room temperature in the syringes, we were able to vary the temperature from one experiment to another. We have checked that in our experimental conditions, room temperature polymerization reactions can be neglected since we obtained the same monomer to initiator height ratios before and after an experiment was done. As shown in Figure 5a, by increasing temperature, the rate also increases as expected. Because of the small size of the droplets and their high surface-area-to-volume ratio, we were capable to polymerize safely high AA concentrations at high temperature, i.e., 5.6 mol·L^{-1} at 98 °C and pH 1.8. This is a very fast reaction which could be difficult to handle at the laboratory by using conventional glassware like Schlenk tubes or jacketed reactors. Moreover, at bigger scales, evacuation of the thermal energy due to the double bond conversion could quickly be an issue. This is enhanced by the high viscosity obtained by using high initial monomer concentrations.

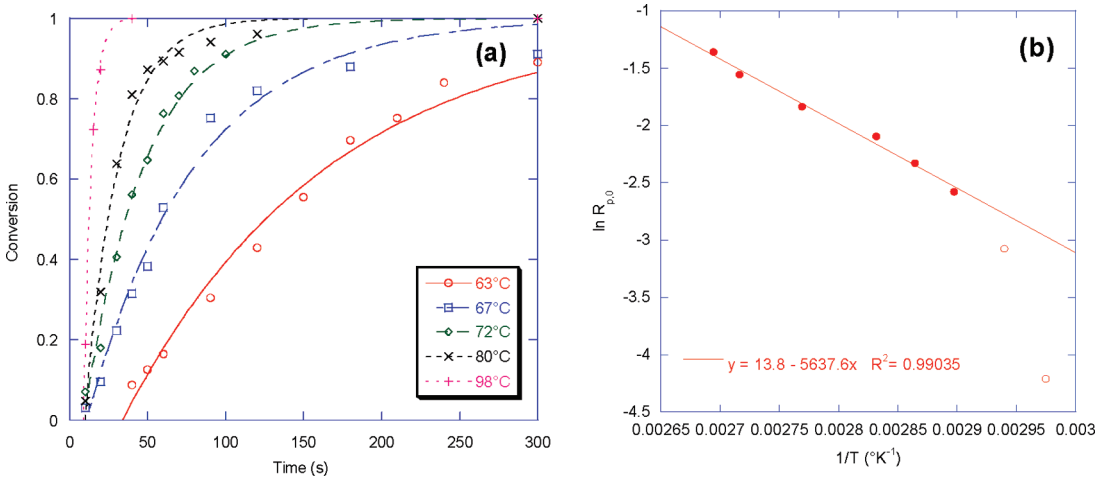

Figure 5. (a) Molar conversions of AA in function of time for several temperatures ($[AA]_0$ = 5.6 mol·L^{-1}, $[I]_0$ = 0.028 mol·L^{-1}, pH 1.8). (b) Temperature dependence of $R_{p,0}$. Only the filled circles were taken into account for the linear fit.

Table 2. Overall Activation Energy for the Rate of Polymerization from the Literature

E_r (kJ mol^{-1})	temperature range (°C)	reference
98.1	36.3−66.8	26
92.1	around 50	27
47.0	72−98	this work
40.1	55−85	28

From the values of $R_{p,0}$ an Arrhenius plot was traced and is shown in Figure 5b. Surprisingly, we did not obtain a strait line meaning the Arrhenius law should not be applied for the whole range of temperatures used, i.e., from 63 to 98 °C. However, it is well-known that AA can be polymerized at lower temperature than 60 °C.[30] As seen in Figure 5b, two different regimes are observed: one for temperatures above 70 °C, and another one for temperatures between 60 to 70 °C where polymerization kinetics are slower and do not allow to the complete conversion of the monomer. Moreover, at temperatures below 60 °C in our experimental conditions, we did not detect any significant polymerization signals by using a residence time of 5 min. This slow polymerization rate was confirmed by heating at 50 °C the reaction mixture within a deoxygenated 2 mL vial. An increase of the viscosity was observed after 60 min only. At temperatures higher than 70 °C, the overall activation energy for the rate of polymerization, E_r, was estimated from the slope of the trace and is 47.0 kJ mol^{-1} with a correlation coefficient of 0.990. This E_r is twice less the value expected when the polymerization reaction is initiated by the thermal dissociation of the initiator (about 90 kJ/mol).[23,24] This is not surprising since the initiation of the aqueous AA polymerization is enhanced by the monomer. However, some published E_r give a quite high value (see Table 2). Interestingly, the curvature observed at about 70 °C in Figure 5b was also detected by Scott and Peppas[26] although the range of temperatures was shifted to lower ones, i.e., from 36 to 67 °C. From the highest part of their Arrhenius plot, one can calculate an E_r of about 49.5 kJ mol^{-1}, which is closer to our measured E_r. On the other hand, Cutié et al. obtained E_r of about 40.1 kJ mol^{-1}, within a temperature range above the curvature limit observed on the graph published by Scott and Peppas, up to 85 °C.[28] Scott and Peppas used a lower concentration than we did, i.e. 30% w/v instead of 40% w/v with roughly the same $[AA]_0/[I]_0$ ratio. It is difficult to accurately know the concentration used by Cutié et al.; however, it does not seem that they used a concentration above 33% w/v. We hence assume the shift in temperatures is due to the difference in solution viscosity. According to the temperature, the solution concentration and the molecular weight of the growing chains, the polymerization rate can dramatically decrease. In other words, the solution become viscous enough to make the propagation step diffusion-limited due to diffusional limitations on the monomer. Thus, the published values of E_r could depend on the range of the concentrations used by the authors. Further works are in progress in the laboratory to fully understand this behavior.

Conclusion

We believe these results validate the usefulness of the droplet-based millifluidic approach to safely synthesize and investigate fast or exothermic polymerization reactions in harsh or "extreme" conditions. It has been shown that the use of droplets as batch microreactors flowing within a heated $^1/_8$ in. o.d. tube can allow investigating quickly and safely AA polymerization reactions at low pH. Since droplet compositions depend only on flow rates, it was easy to screen different experimental conditions, including those which could not be studied in conventional batch reactors (i.e., high monomer concentrations and temperatures; 40% w/v and 98 °C). Hence, this approach can be used as a powerful high throughput screening (HTS) tool. Moreover, coupled with appropriate and sensitive analytical systems, basic kinetic data can be obtained *in line* through the wall of the transparent tube. By using Raman spectrometry and the time-space equivalence specific to the use of droplets, we were capable to monitor molar conversion and monomer concentration in function of time. Thus, we were able to verify the higher than first order kinetics in initial monomer concentration and a $^1/_2$ dependence in initial initiator concentration. We were also able to measure the overall activation energy for the rate of polymerization at high temperatures, i.e., when the propagation step is not diffusion-limited. In conclusion, droplet-based millifluidics seems to be a promising HTS approach for investigating kinetics and possibly tailoring polymer properties. Further works are in progress at the laboratory to generate more complex polymeric structures and to investigate copolymerization reactions by using this approach.

Acknowledgment. Supports from the CNRS, Rhodia and the University of Bordeaux 1 are gratefully acknowledged. The authors also thank Dr. Carine Rosenfeld and Dr. James Wilson (Rhodia) for fruitful discussions and Marie Dietemann for her kind help during her internship.

References and Notes

(1) Huebner, A.; Sharma, S.; Srisa-Art, M.; Hollfelder, F.; Edel, J. B.; DeMello, A. J. *Lab Chip* **2008**, *8*, 1244–1254.

(2) Song, H.; Chen, D. L.; Ismagilov, R. F. *Angew. Chem., Int. Ed.* **2006**, *45*, 7336–7356.
(3) Dendukuri, D.; Doyle, P. S. *Adv. Mater.* **2009**, *21*, 4071–4086.
(4) Steinbacher, J. L.; McQuade, D. T. *J. Polym. Sci., Part A: Polym. Chem.* **2006**, *44*, 6505–6533.
(5) Sarrazin, F. M.S. Thesis, Institut National Polytechnique de Toulouse: Toulouse, France, 2006
(6) Aubin, J.; Ferrando, M.; Jiricny, V. *Chem. Eng. Sci.* **2010**, *65*, 2065–2093.
(7) Iwasaki, T.; Yoshida, J. *Macromolecules* **2005**, *38*, 1159–1163.
(8) Song, H.; Tice, J. D.; Ismagilov, R. F. *Angew. Chem., Int. Ed.* **2003**, *42*, 768–772.
(9) Barnes, S. E.; Cygan, Z. T.; Yates, J. K.; Beers, K. L.; Amis, E. J. *Analyst* **2006**, *131*, 1027–1033.
(10) Song, H.; Ismagilov, R. F. *J. Am. Chem. Soc.* **2003**, *125*, 14613–14619.
(11) Pavageau, B.; Christobal, G.; Rabih, R.; Vuong, C. T. WO2008043860, 2008, Rhodia operation.
(12) Panizza, P.; Christobal, G.; Pavageau, B.; Colin, A. WO2008043922, 2008, Rhodia operation and University of Bordeaux 1.
(13) Panizza, P.; Engl, W.; Pavageau, B.; Galinat, S. FR2907030, 2008, Rhodia Recherches et Technologies and Université de Bordeaux 1.
(14) Engl, W.; Tachibana, M.; Panizza, P.; Backov, R. *Int. J. Multiphase Flow* **2007**, *33*, 897–903.
(15) Tachibana, M.; Engl, W.; Panizza, P.; Deleuze, H.; Lecommandoux, S.; Ushiki, H.; Backov, R. *Chem. Eng. Process.* **2008**, *47*, 1317–1322.
(16) Panizza, P.; Engl, W.; Hany, C.; Backov, R. *Colloids Surf. A: Physicochem. Eng. Aspects* **2008**, *312*, 24–31.
(17) Engl, W.; Tachibana, M.; Colin, A.; Panizza, P. *Chem. Eng. Sci.* **2008**, *63*, 1692–1695.
(18) Quevedo, E.; Steinbacher, J.; McQuade, D. T. *J. Am. Chem. Soc.* **2005**, *127*, 10498–10499.
(19) Serra, C.; Berton, N.; Bouquey, M.; Prat, L.; Hadziioannou, G. *Langmuir* **2007**, *23*, 7745–7750.
(20) Gokmen, M. T.; Van Camp, W.; Colver, P. J.; Bon, S. A. F.; Du Prez, F. E. *Macromolecules* **2009**, *42*, 9289–9294.
(21) Cygan, Z. T.; Cabral, J. T.; Beers, K. L.; Amis, E. J. *Langmuir* **2005**, *21*, 3629–3634.
(22) Guan, G.; Kusakabe, K.; Moriyama, K.; Sakurai, N. *Ind. Eng. Chem. Res.* **2009**, *48*, 1357–1363.
(23) Odian, G. *Principles of Polymerization*, 4th ed.; Odian, G., Ed.; John Wiley & Sons, Inc.: Hoboken, NJ, 2004.
(24) Dotson, N. A., Galvan, R., Laurence, R. L., Tireel, M. *Polymerization Process Modelling*: John Wiley & Sons, Inc.: New York, 1996.
(25) Çatalgil-Giz, H.; Giz, A.; Alb, A. M.; Reed, W. F. *J. Appl. Polym. Sci.* **2004**, *91*, 13521359.
(26) Scott, R. A.; Peppas, N. A. *AIChE J.* **1997**, *43*, 135–144.
(27) Manickam, S. P.; Venkatarao, K.; Subbaratnam, N. R. *Eur. Polym. J.* **1979**, *15*, 483–487.
(28) Cutié, S. S.; Smith, P. B.; Henton, D. E.; Staples, T. L.; Powell, C. *J. Polym. Sci., Part B: Polym. Phys.* **1997**, *35*, 2029–2047.
(29) Henton, D. E.; Powell, C.; Reim, R. E. *J. Appl. Polym. Sci.* **1997**, *64*, 561–600.
(30) Kabanov, V. A.; Topchiev, D. A.; Karaputadze, T. M.; Mkrtchian, L. A. *Eur. Polym. J.* **1975**, *11*, 153–159.